**Bulletin of Electrical Engineering and Informatics**
Vol. 14, No. 6, December 2025, pp. 4198~4207
ISSN: 2302-9285, DOI: 10.11591/eei.v14i6.9634


# Improved power quality and reduced losses in DFIG-based WECS using third-order sliding mode control

**Abdelaziz Belhait[1], Messaoud Louafi[1], Sihem Ghoudelbourk[2]**
[1]Department of Electromechanics, Mining Institute, Environmental Laboratory, Echahid Cheikh Larbi Tebessi University, Tebessa, Algeria
[2]Department of Electrical Engineering, Faculty of Technology, Badji Mokhtar Annaba University, Annaba, Algeria

**Article Info**

***Article history:***

Received Dec 1, 2024
Revised Aug 21, 2025
Accepted Sep 27, 2025

***Keywords:***

Doubly fed induction generator
Electrical losses
Super-twisting sliding mode control
Third-order sliding mode control
Total harmonic distortion
Wind energy conversion systems

**ABSTRACT**

The study presents a comparative analysis of two advanced high-order sliding mode control (HOSMC) strategies—super-twisting sliding mode control (STSMC) and third-order sliding mode control (TOSMC)—for enhancing the performance of doubly-fed induction generator (DFIG)-based wind energy conversion systems (WECS). The key goals are to maximize energy efficiency, minimize the total harmonic distortion (THD) in the stator current, and reduce electrical losses within the system. Both control strategies are integrated into a direct field-oriented control (DFOC) scheme using space vector modulation (SVM) to improve dynamic response and control accuracy. MATLAB/Simulink simulations show that TOSMC consistently outperforms STSMC in multiple performance aspects. TOSMC ensures better energy efficiency through precise tracking of active and reactive power references while mitigating transient oscillations (chattering effects). Furthermore, TOSMC significantly reduces harmonic distortion, achieving a THD of 0.21%, compared to 0.33% for STSMC, and surpasses conventional controllers, which exhibit a minimum recorded THD of approximately 0.46%. The mitigation of transient phenomena also contributes to reduced switching losses and ohmic heating, thereby enhancing the generator's thermal stability and overall reliability.



***Corresponding Author:***

Abdelaziz Belhait
Department of Electromechanics, Mining Institute, Environmental Laboratory
Echahid Cheikh Larbi Tebessi University
Tebessa 12000, Algeria
Email: abdelaziz.belhait@univ-tebessa.dz

## 1. INTRODUCTION

Renewable energy sources have become central to the global energy transition, with wind energy standing out due to its rapid development and increasing share in the energy mix [1]. Among various wind-based generation systems, the doubly-fed induction generator (DFIG) has emerged as one of the most widely adopted technologies in wind energy conversion systems (WECS), primarily due to its reduced cost, high efficiency, and controllability under varying wind conditions [2].

However, despite these advantages, DFIG-based systems are challenged by elevated levels of total harmonic distortion (THD) in the stator currents, which significantly degrade the quality of power, increase energy losses, and lower overall system efficiency [3]. To overcome these issues, several control strategies have been explored, such as direct power control (DPC) [4], direct field oriented control (DFOC) [5], and indirect field oriented control (IFOC) [6]. Among them, DFOC has demonstrated promising results, offering a good balance between dynamic performance and implementation simplicity.

To enhance the robustness and dynamic response of the system, sliding mode control (SMC) techniques have been introduced [7]. In particular, the super-twisting sliding mode control (STSMC) approach provides improved fault tolerance and disturbance rejection [8], yet it is not free from drawbacks such as increased ripple and persistent THD levels [9]. To address these limitations, this study proposes a more advanced nonlinear control approach: third-order sliding mode control (TOSMC) [10], which is a higher-order extension of conventional SMC.

TOSMC is known for its ability to reduce the chattering effect, a key factor contributing to THD and control instability in power systems [11]. By incorporating higher-order derivatives, the TOSMC method significantly smooths control signals, resulting in reduced power fluctuations and energy losses.

This paper presents the integration of TOSMC within the DFOC framework, introducing a novel hybrid control strategy named DFOC-TOSMC. The key contributions of this work are as follows:

- Development of a DFOC-TOSMC controller to reduce THD and enhance transient performance;
- Comparative analysis with existing DFOC-STSMC strategies to highlight performance improvement;
- Simulation-based validation using MATLAB/Simulink to evaluate the effectiveness under varying operating conditions.

The rest of this manuscript is organized as follows: section 2 presents the modelling of the wind turbine and the DFIG. Section 3 describes the control strategy based on (STSMC), along with the proposed strategy using (TOSMC). Section 4 discusses the simulation results and analyzes the performance of the proposed approach. Finally, section 5 concludes the paper and suggests directions for future research.

## 2. MATHEMATICAL MODEL OF WIND ENERGY CONVERSION SYSTEM

### 2.1. Mathematical model of wind turbine

In (1) represents the aerodynamic power produced by the wind [12]:

$$p_t = \frac{1}{2}\rho\pi {R_t}^2 V^3 C_p(\lambda,\beta) \quad (1)$$

Where the air density is denoted by $\rho$=1,225 kg/m³, the blade radius is represented by $R_t$ in meters, and the wind speed is represented by $V$ in (m/s). The performance coefficient, $C_p$ depends on the tip-speed ratio ($\lambda$) and the pitch angle ($\beta$).

The tip-speed ratio (λ) represents the ratio between the linear velocity of the blades ($\Omega_t$) and the wind speed ($V$):

$$\lambda = \frac{\Omega_t . R_t}{V} \quad (2)$$

### 2.2. Mathematical model of doubly-fed induction generator

To present the mathematical model of the DFIG, the Park transformation is typically used in the $d-q$ reference frame [13], where the stator and rotor voltages are given by (3):

$$\begin{cases} V_{ds} = R_s i_{ds} + \frac{d\varphi_{ds}}{dt} - \omega_s \varphi_{qs} \\ V_{qs} = R_s i_{qs} + \frac{d\varphi_{qs}}{dt} + \omega_s \varphi_{ds} \\ V_{dr} = R_r i_{dr} + \frac{d\varphi_{dr}}{dt} - \omega_r \varphi_{qr} \\ V_{qr} = R_r i_{qr} + \frac{d\varphi_{qr}}{dt} + \omega_r \varphi_{dr} \end{cases} \quad (3)$$

The flux of the stator and rotor of the DFIG is represented by (4):

$$\begin{cases} \varphi_{ds} = l_s i_{ds} + M i_{dr} \\ \varphi_{qs} = l_s i_{qs} + M l_r i_{qr} \\ \varphi_{dr} = l_r i_{dr} + M i_{ds} \\ \varphi_{qr} = l_r i_{qr} + M i_{qs} \end{cases} \quad (4)$$

The stator and rotor voltages are represented, respectively, by the values of $V_{ds}$, $V_{qs}$, $V_{dr}$, and $V_{qr}$ on the $d-q$ axis. The stator and rotor currents are represented by the currents $i_{ds}$, $i_{qs}$, $i_{dr}$, and $i_{qr}$ while the stator and rotor flux components are represented by $\varphi_{ds}$, $\varphi_{qs}$, $\varphi_{dr}$, and $\varphi_{qr}$. $R_r$ and $R_s$ stand for the resistances of the rotor and stator windings on the $d-q$ axis. The self-inductance of the rotor, the

self-inductance of the stator, and the mutual inductance between two coils are indicated by the values $L_s$, $L_r$, and $M$ respectively, utilising $\omega_r = \omega_s - p.\Omega_g$ . In (5) represents the active and reactive powers of the stator:

$$\begin{cases} P_s = \frac{3}{2}(V_{ds}i_{ds} + V_{qs}i_{qs}) \\ Q_s = \frac{3}{2}(V_{qs}i_{ds} - V_{ds}i_{qs}) \end{cases} \quad (5)$$

by using the stator flux orientation technique and selecting a Park reference frame linked to the stator flux, while neglecting the stator resistance $R_S$.

$$\varphi=\varphi_{ds}=\varphi_s \text{ and } \varphi_{qs}=0 \quad (6)$$

We obtain the stator voltages and currents, respectively, as (7) and (8) [14]:

$$\begin{cases} v_{ds} = 0 \\ v_{qs} = v_s = \omega_s\varphi_s \end{cases} \quad (7)$$

$$\begin{cases} i_{ds} = \frac{\varphi_s}{l_s} - \frac{M}{l_s}i_{dr} \\ i_{qs} = -\frac{M}{l_s}i_{qr} \end{cases} \quad (8)$$

Furthermore, the equations for active and reactive power can be expressed in terms of the rotor current components $I_{dr}$ and $I_{qr}$, as (9):

$$\begin{cases} P_s = \frac{3}{2}\left(-V_s\frac{M}{l_s}i_{qr}\right) \\ Q_s = \frac{3}{2}(-V_s\frac{M}{l_s}i_{dr} + \frac{{V_s}^2}{l_s\omega_s}) \end{cases} \quad (9)$$

The rotor voltage equations can be simplified as (10) [15]:

$$\begin{cases} V_{dr} = R_r i_{dr} + \sigma l_r\frac{dI_{dr}}{dt} - \sigma l_r\omega_r i_{qr} \\ V_{qr} = R_r i_{qr} + \sigma l_r\frac{dI_{qr}}{dt} + \sigma l_r\omega_r i_{dr} + \omega_r\frac{M}{Ls}\varphi_s \end{cases} \quad (10)$$

where:

$$\sigma = 1 - \frac{M^2}{l_r.Ls} \quad (11)$$

## 3. COMMAND TECHNIQUES OF THE DOUBLY-FED INDUCTION GENERATOR

In this section, we compare two controllers, the STSMC and the TOSMC, to improve energy efficiency and reduce electrical losses in the wind generation system based on the DFIG. Both methods rely on reduce the chattering phenomenon to enhance the characteristics of direct field-oriented control (DFOC).

### 3.1. Direct field orientation control

The DFOC technique is a control method that simplifies the system by neglecting the coupling terms between the stator and rotor fluxes. This makes it easy to implement and based on a simplified algorithm. In this control strategy, two independent regulators are installed—one for each axis—to separately control active and reactive power, as described in [6]. Figure 1 illustrates the block diagram of the DFOC method, which utilizes two PI-type controllers [5].

### 3.2. Super-twisting sliding mode control-direct field orientation

Despite the simplicity of the DFOC technique, it has several limitations that hinder its effectiveness, especially when compared to the indirect field-oriented control (IFOC) method [5]. These drawbacks include significant power ripple and high THD, which result in increased electrical losses. To address these challenges, the STSMC technique replaces the traditional PI regulator block. The design of this approach is shown in Figure 2.

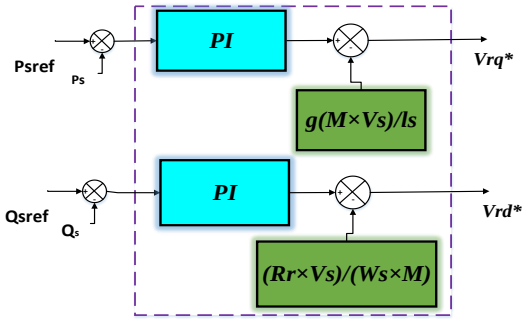


Figure 1. Direct FOC technique

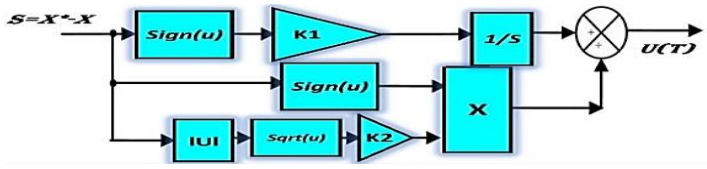


Figure 2. The STSMC technique

The control law $U(t)$ for a dynamic system is defined as a combination of two components: the primary control $u1(t)$ and the corrective control $u2(t)$, as (12) [16], [17]:

$$u = u1 + u2 \tag{12}$$

In the context of the super-twisting sliding mode controller (STSMC), the two control components are defined as follows:

$$u1 = -k1 \int sign(s)dt \quad , \quad u2(t) = -\mathrm{k2}.\ |S|^{\frac{1}{2}}\mathrm{sign(s)}$$

where $K1$ and $K2$ are positive constants.

In (13) represents the super-twisting (ST) control law, which is integrated into the direct field-oriented control (DFOC) scheme [18]:

$$u(t) = -\mathrm{k1}.\ |S|^{1/2}\mathrm{sign(s)}\ - \mathrm{k2}\int \mathrm{sign(s)dt} \tag{13}$$

### 3.3. Third-order sliding mode control-direct field-oriented control

A new method is introduced to reduce chattering phenomena, building on the STSMC algorithm [19]. This approach, known as TOSMC, is a nonlinear method that offers simplicity and ease of implementation, key advantages over traditional SMC methods. TOSMC effectively mitigates the drawbacks of chattering and enhances energy production in wind systems [10]. The implementation of the TOSMC controller marks a significant advancement in this field. To enhance the performance of the DFOC strategy, the TOSMC technique replaces the STSMC control, leading to improved dynamic response. This integration reduces THD and electrical losses, making it a valuable contribution to the efficiency of wind power generation. In (14) represents the TOSMC technique used:

$$u(t) = k1.sign(s)\ + k2\int sign(s)dt\ + k3\sqrt{|s|}\,.sign(s) \tag{14}$$

with $k1$ and $K2$ and $K3$ being positive constants.

Figure 3 presents the structure of the proposed TOSMC regulator. The TOSMC method is detailed in [20].

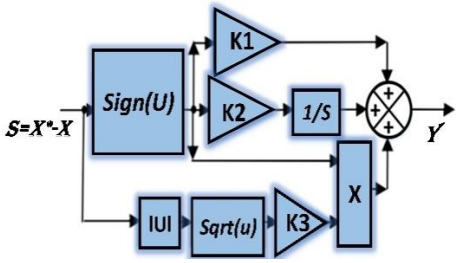


Figure 3. The TOSMC technique

## 4. RESULTS AND DISCUSSION

To examine and validate the effectiveness of the two high-order sliding mode control (HOSMC) techniques (STSMC and TOSMC), numerical simulations were conducted in MATLAB. The system parameters are detailed in Table 1. Figure 4 illustrates the proposed approach for power control, which integrates DFOC and space vector modulation (SVM) in a WECS based on a DFIG.

Table 1. parameters of WT-DFIG

| Parameters | Value |
|---|---|
| Nominal power | 10 kW |
| Blade radius ($R_t$) | 3 m |
| Gearbox gain ($G$) | 5.4 |
| Moment of inertia ($Jt$) | 0.042 Kg.m$^2$ |
| Friction coefficient ($ft$) | 0.017 N.m/s |
| Air density ($\rho$) | 1.225 Kg/m$^3$ |
| Tip speed ratio ($\lambda$) | 2.8 |
| Stator frequency ($f$) | 50 Hz |
| Resistance of stator ($R_s$) | 1.518 Ω |
| Resistance of rotor ($R_r$) | 1.247 Ω |
| Inductance of stator ($l_s$) | 0.0921 H |
| Mutual inductance ($M$) | 0.0696 H |
| Inductance of rotor ($l_r$) | 0.0640 H |

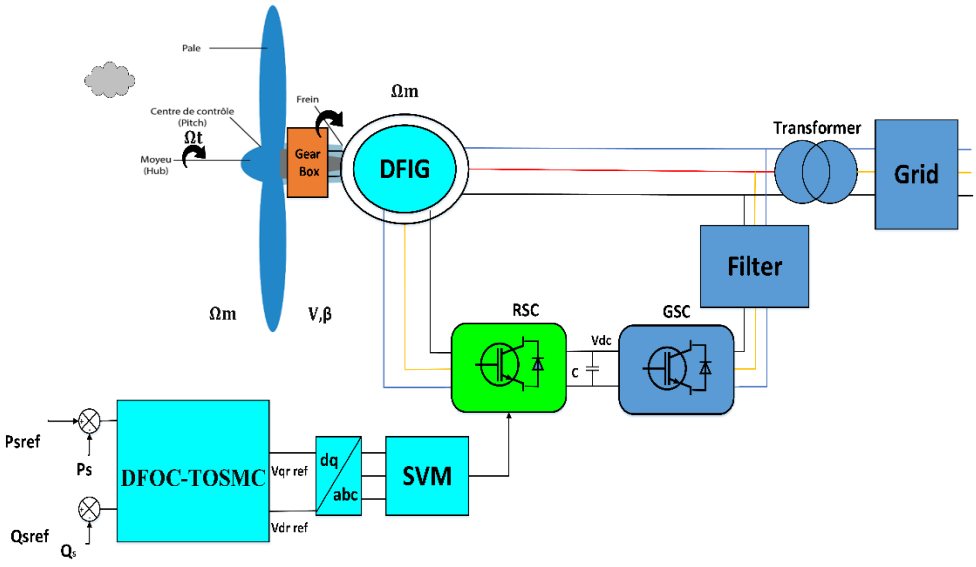


Figure 4. DFOC strategy with TOSMC controller

The two controllers applied to DFOC are clearly compared through the results shown in Figures 5-8. Figure 5 shows the step-shaped wind profile used as input. Under this wind profile, the active and reactive power responses are presented in Figure 6.

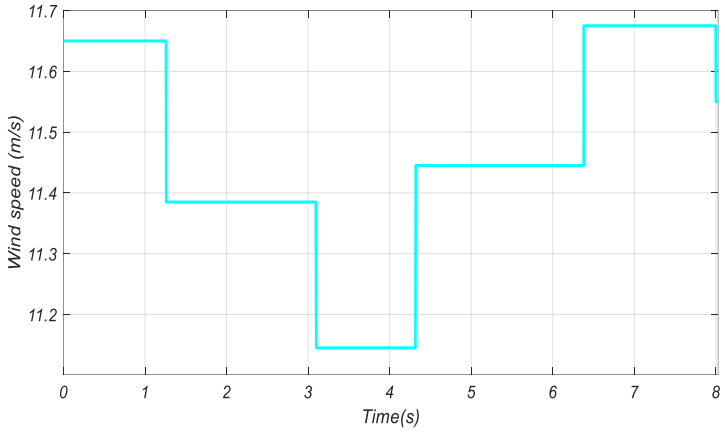


Figure 5. Wind speed profile step variation

Figure 6(a) presents the active power. The best performance is achieved with the TOSMC controller, which exhibits less fluctuation compared to the reference, resulting in a stable and accurate response. In contrast, before stabilizing the power, the STSMC shows notable initial oscillations with a longer adjustment period.

Regarding reactive power (Figure 6(b)), the reference values are closely followed by the TOSMC control with minimal deviation and indicating precise regulation. However, the STSMC displays larger variations initially, with a period of instability before gradually aligning with the reference. Therefore, to maintain energy quality under fluctuating conditions, the TOSMC can be considered superior.

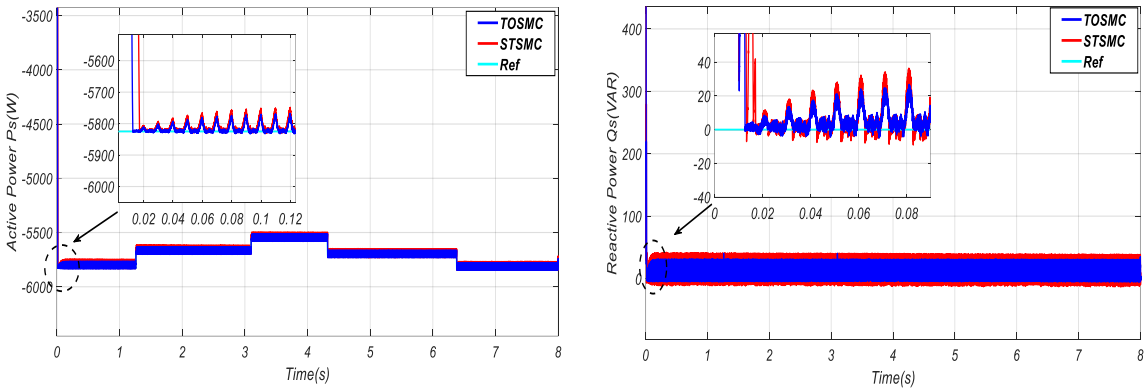


(a) (b)

Figure 6. Power response: (a) active power (Ps) and (b) reactive power (Qs)

The stator current curves (Isa) shown in Figure 7 indicate that both control strategies—TOSMC and STSMC—exhibit nearly identical performance, with an almost perfect overlap observed in Figure 7(a). This suggests equivalent effectiveness in regulating the stator current. However, a closer inspection in the zoomed view (Figure 7(b)) reveals a slight advantage in favor of the TOSMC approach. Consequently, both methods prove effective in maintaining low electrical losses, which is a critical factor in enhancing the efficiency of energy generation systems.

Finally, Figure 8 compares the THD for both control methods. The STSMC method (Figure 8(a)) yields a THD of 0.33%, while the TOSMC method (Figure 8(b)) presents a lower THD of 0.21%. The observed reduction in THD using TOSMC is attributed to its higher-order structure, which enhances the smoothness of the control signal and significantly reduces chattering. Unlike traditional STSMC, the third-order sliding mode introduces additional filtering dynamics that effectively suppress high-frequency switching components, thereby minimizing harmonic injection into the system. As a result, the TOSMC controller proves more efficient in reducing THD and, by extension, in lowering electrical losses in DFIG-based WECS.

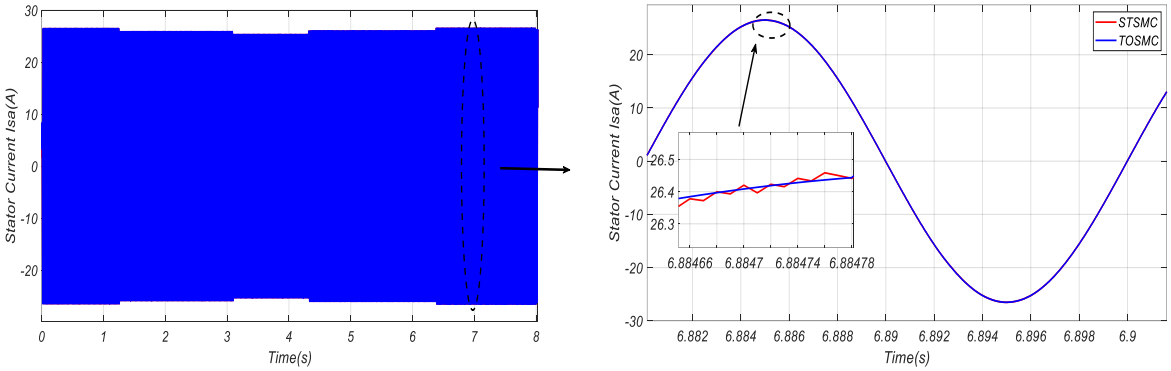


(a) (b)

Figure 7. Stator current (Isa): (a) overall response and (b) zoomed-in view of the stator current

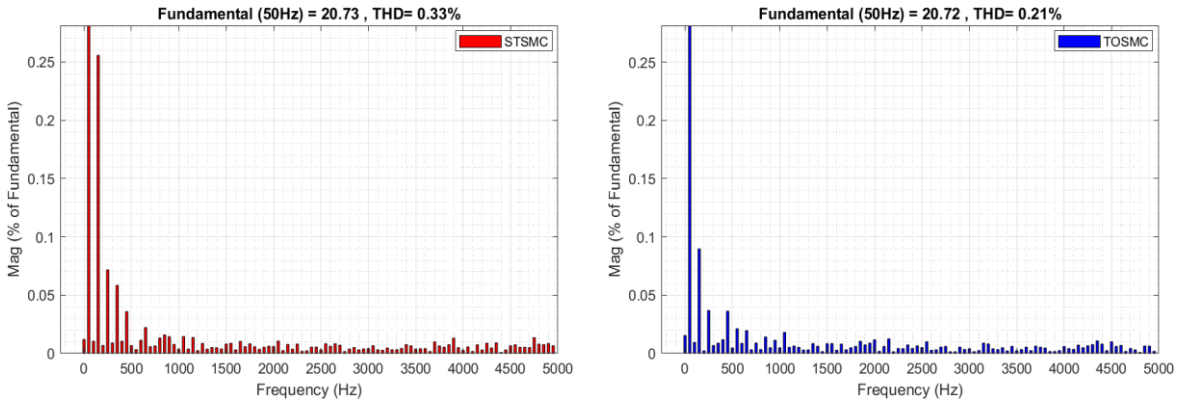


(a) (b)

Figure 8. THD analysis of the stator current: (a) THD values for STSMC and (b) THD values for TOSMC

Table 2 presents a comparative evaluation of the TOSMC and STSMC control strategies. The TOSMC approach demonstrates superior performance over the STSMC in regulating DFIG dynamics. TOSMC provides faster stabilisation, drastically reduces overshoots in both active and reactive power, and minimizes reactive energy consumption, all while maintaining comparable total energy production. These improvements confirm TOSMC's robustness and energy efficiency, positioning it as a promising control strategy for high-performance power systems.

Table 2. A comparative analysis of the stabilisation time, overshoot, and total energy of STSMC and TOSMC

| Method | Signal | Stabilisation time | Overshoot | Energy produced |
|---|---|---|---|---|
| STSMC | Ps (W) | 23 | 5,824 | 37,200 |
| | Qs (VAR) | 18 | 19.58 | 125 |
| TOSMC | Ps (W) | 17 | 720 | 37,300 |
| | Qs (VAR) | 10 | 5 | 11 |

The comparison of THD values presented in Table 3 indicates that the DFOC-TOSMC and DFOC-STSMC strategies outperform the other methods, achieving THD values of 0.21% (STSMC–Figure 8(a)) and 0.33% (TOSMC–Figure 8(b)), respectively, thereby demonstrating excellent electrical signal quality, particularly with the proposed DFOC-TOSMC method. Meanwhile, other approaches such as DPC-ANFIS-STSMC also yield good results, maintaining THD values below 0.5%. In contrast, the ISMC controller exhibits the highest THD at 1.33%, reflecting greater electrical losses and reduced signal quality.

Table 3. Comparative table of the proposed control method and other control techniques

| Strategies | THD (%) | References |
|---|---|---|
| DPC with STSMC | 0.85 | [21] |
| DPC ANFIS-STSMC | 0.46 | [22] |
| ISMC | 1.33 | [23] |
| TOSMC technique | 0.83 | [10] |
| DRAPC method | 1.08 | [24] |
| DPC-NSTSMC-SVM | 0.99 | [25] |
| DFOC-STSMC | 0.33 | Designed strategies |
| DFOC-TOSMC | 0.21 | |

## 5. CONCLUSION

This study aimed to evaluate and compare the performance of advanced higher-order sliding mode controllers—namely, STSMC and TOSMC—within a DFIG-based WECS. The results confirmed that both controllers significantly improve power quality and system efficiency by reducing THD with TOSMC demonstrating superior dynamic response and robustness under varying wind conditions.

These outcomes fulfill the research objective of enhancing electrical performance in variable-speed wind systems through advanced nonlinear control strategies. The findings suggest that applying TOSMC within DFOC architectures can reduce electrical losses, improve grid compliance, and potentially lower maintenance costs—offering tangible benefits for industrial-scale wind power applications.

However, the study is limited to simulation-based validation under standard test conditions. Future work should focus on experimental validation in real-time environments and explore the integration of TOSMC in hybrid renewable systems, particularly wind–solar configurations, to expand its applicability in diverse operating contexts.

## FUNDING INFORMATION

Authors state no funding involved.

## AUTHOR CONTRIBUTIONS STATEMENT

This journal uses the Contributor Roles Taxonomy (CRediT) to recognize individual author contributions, reduce authorship disputes, and facilitate collaboration.

| Name of Author | C | M | So | Va | Fo | I | R | D | O | E | Vi | Su | P | Fu |
|---|---|---|---|---|---|---|---|---|---|---|---|---|---|---|
| Abdelaziz Belhait | ✓ | ✓ | ✓ | ✓ | ✓ | ✓ | ✓ | ✓ | ✓ | ✓ | | | ✓ | ✓ |
| Messaoud Louafi | | | | | | ✓ | | ✓ | ✓ | ✓ | ✓ | ✓ | | |
| Sihem Ghoudelbourk | ✓ | | ✓ | ✓ | ✓ | ✓ | ✓ | | | ✓ | ✓ | | ✓ | ✓ |

C : **C**onceptualization
M : **M**ethodology
So : **So**ftware
Va : **Va**lidation
Fo : **Fo**rmal analysis
I : **I**nvestigation
R : **R**esources
D : **D**ata Curation
O : Writing -**O**riginal Draft
E : Writing - Review &**E**diting
Vi : **Vi**sualization
Su : **Su**pervision
P : **P**roject administration
Fu : **Fu**nding acquisition

## CONFLICT OF INTEREST STATEMENT

Authors state no conflict of interest.

## INFORMED CONSENT

We have obtained informed consent from all individuals included in this study.

## DATA AVAILABILITY

Data availability is not applicable to this paper as no new data were created or analyzed in this study.

## REFERENCES


[1] D. Yoo, S. Kang, G. Jang, and S. Jung, "Development of reactive power allocation method for radial structure wind farm considering multiple connections," *Electronics*, vol. 11, no. 14, Jul. 2022, doi: 10.3390/electronics11142176.

[2] A. Dannier, E. Fedele, I. Spina, and G. Brando, "Doubly-fed induction generator (DFIG) in connected or weak grids for turbine-based wind energy conversion system," *Energies*, vol. 15, no. 17, 2022, doi: 10.3390/en15176402.

[3] K. Sabzevari *et al.*, "Low-voltage ride-through capability in a DFIG using FO-PID and RCO techniques under symmetrical and asymmetrical faults," *Scientific Reports*, vol. 13, 2023, doi: 10.1038/s41598-023-44332-y.

[4] M. Mazouz, B. Sebti, and C. Ilhami, "DPC-SVM of DFIG using fuzzy second order sliding mode approach," *International Journal of Smart Grid (IJSmartGrid)*, vol. 5, no. 4, pp. 174–182, 2021, doi: 10.20508/ijsmartgrid.v5i4.219.g178.

[5] A. Chahbi, M. Yessef, A. Amharech, and H. Ameziane, "Robust control of doubly fed induction generator based on direct field oriented control," *2025 17th International Conference on Electronics, Computers and Artificial Intelligence (ECAI)*, Bucharest, Romania, Jun. 2025, pp. 1–5, doi: 10.1109/ECAI65401.2025.11095617.

[6] B. Desalegn, D. Gebeyehu, and B. Tamrat, "Smoothing electric power production with DFIG-based wind energy conversion technology by employing hybrid controller model," *Energy Reports*, vol. 10, pp. 38–60, 2023, doi: 10.1016/j.egyr.2023.06.004

[7] H. Itouchene, Z. Boudries, and F. Amrane, "Improved power control based variable speed wind-turbine DFIG under hard work conditions: Application of sliding mode theory," *Periodica Polytechnica Electrical Engineering and Computer Science*, vol. 68, no. 4, pp. 392–412, 2024, doi: 10.3311/PPee.36760.

[8] I. Sami, S. Ullah, S. U. Amin, A. Al-Durra, N. Ullah, and J. Ro, "Convergence enhancement of super-twisting sliding mode control using artificial neural network for DFIG-based wind energy conversion systems," *IEEE Access*, vol. 10, pp. 97625–97641, 2022, doi: 10.1109/ACCESS.2022.3205632

[9] D. Daou, S. Farhat, Y. Dbaghi, F. E. Nadir, C. Touiza, and S. Mouslim, "Comparative Analysis of SMC and PI Controls in DFIG Wind Systems," *2024 4th International Conference on Innovative Research in Applied Science, Engineering and Technology (IRASET)*, FEZ, Morocco, 2024, pp. 1-12, doi: 10.1109/IRASET60544.2024.10548962.

[10] S. Kadi, H. Benbouhenni, E. Abdelkarim, K. Imarazene, and E. M. Berkouk, "Implementation of third-order sliding mode for power control and maximum power point tracking in DFIG-based wind energy systems," *Energy Reports*, vol. 10, pp. 3561–3579, 2023, doi: 10.1016/j.egyr.2023.09.187.

[11] A. Dendouga, A. Dendouga, and N. Essounbouli, "High performance of variable-pitch wind system based on a direct matrix converter-fed DFIG using third order sliding mode control," *Wind Engineering*, vol. 48, no. 3, pp. 325–348, 2024, doi: 10.1177/0309524X231199435.

[12] A. Milles *et al.*, "Optimizing PI Regulators for DFIGs in Wind Energy Using Artificial Intelligence," *2024 2nd International Conference on Electrical Engineering and Automatic Control (ICEEAC)*, May 2024, pp. 1–6, doi: 10.1109/ICEEAC61226.2024.10576462.

[13] H. Hichem, T. A. Abderrazak, A. Iliace, M. S. Bendelhoum, and B. Abdelkrim, "A new robust SIDA-PBC approach to control a DFIG," *Bulletin of Electrical Engineering and Informatics*, vol. 12, no. 3, pp. 1310–1317, 2023, doi: 10.11591/eei.v12i3.2155.

[14] A. Belhait, M. Louafi, S. Ghoudelbourk, G. Boukhalfa, and A. Milles, "Comparative Study of DPC and Backstepping Controllers in a Doubly Fed Induction Generator-Based Wind Energy Conversion System," *Power System and Distributed Renewable Energy Journal (PSDREJ)*, vol. 2, no. 1, Apr. 2025, doi: 10.59684/psdrej.v2i01.

[15] H. Abdelli, A. Mezouar, M. Bendjebbar, and K. Belgacem, "Synthesis of SMC algorithms applied to wind generator," *International Journal of Power Electronics and Drive Systems (IJPEDS)*, vol. 12, no. 1, pp. 404–412, 2021, doi: 10.11591/ijpeds.v12.i1.pp404-412.

[16] M. Ilyas, A. Khan, Z. Ahmed, D. W. Jung, and R. Khan, "Altitude stabilization of VTOL system with nonlinear control strategy," *IEEE Access*, vol. 13, pp. 1–10, 2025, doi: 10.1109/ACCESS.2025.3544133.

[17] A. K. A. Zahra and W. A. Wali, "Design of optimal STSMC method based on FPGA to track the trajectory of 2-DOF robot manipulator," *International Journal of Electrical and Electronic Engineering (IJEEE)*, vol. 20, no. 2, 2024, doi: 10.37917/ijeee.20.2.19.

[18] A. Belhait, M. Louafi, S. Ghoudelbourk, G. Boukhalfa, and A. Milles, "Comparative study of three types of MPPT controllers for a wind energy conversion system," in *2024 2nd International Conference on Electrical Engineering and Automatic Control (ICEEAC)*, Setif, Algeria, 2024, pp. 1-6, doi: 10.1109/ICEEAC61226.2024.10576568.

[19] D. K. Wassie, L. N. Lemma, and A. T. Kassie, "HGAPSO based third order-SMC, ST-SMC, and SMC strategy for UAV control: A comparative analysis," *IEEE Access*, vol. 13, pp. 1–12, 2025, doi: 10.1109/ACCESS.2025.3553146.

[20] K. Walid, M. Sofiane, H. Benbouhenni, G. Hamza, and T. Es-saadi, "Application of third-order sliding mode controller to improve the maximum power point for the photovoltaic system," *Energy Reports*, vol. 9, pp. 5372–5383, 2023, doi: 10.1016/j.egyr.2023.04.366.

[21] A. Hadoune *et al.*, "Optimizing direct power control of DFIG-based WECS using super-twisting algorithm under real wind profile," *Frontiers in Energy Research*, vol. 11, 2023, doi: 10.3389/fenrg.2023.1261902.

[22] H. Benbouhenni, Z. Boudjema, and A. Belaidi, "DPC based on ANFIS super-twisting sliding mode algorithm of a doubly-fed induction generator for wind energy system," *Journal Européen des Systèmes Automatisés*, vol. 53, no. 1, pp. 69–80, 2020, doi: 10.18280/jesa.530109.

[23] H. Chojaa, A. Derouich, O. Zamzoum, A. Watil, M. Taoussi, and A. Y. Abdelaziz, "Robust control of DFIG-based WECS integrating an energy storage system with intelligent MPPT under a real wind profile," *IEEE Access*, vol. 11, pp. 90065–90083, 2023, doi: 10.1109/ACCESS.2023.3306722.

[24] H. Benbouhenni and S. Lemdani, "Combining synergetic control and super twisting algorithm to reduce the active power undulations of doubly fed induction generator for dual-rotor wind turbine system," *Electrical Engineering & Electromechanics*, no. 3, pp. 8–17, 2021, doi: 10.20998/2074-272X.2021.3.02.

[25] M. Yessef, H. Benbouhenni, M. Taoussi, A. Lagrioui, I. Colak, and A. Mobayen, "Real-time validation of intelligent super-twisting sliding mode control for variable-speed DFIG using dSPACE 1104 board," *IEEE Access*, vol. 12, pp. 31892–31915, 2024, doi: 10.1109/ACCESS.2024.3367828.

## BIOGRAPHIES OF AUTHORS

**Abdelaziz Belhait** was born in Annaba, Algeria. He obtained his Master's degree in Electromechanics in 2020. Currently, he is a Ph.D. student at the Environment Laboratory, Department of Electromechanical, Mining Institute, University of Larbi Tebessi, Tebessa, Algeria. His research interests include the application of robust control for optimizing generation systems in wind turbine systems. He can be contacted at email: abdelaziz.belhait@univ-tebessa.dz.

**Messaoud Louafi** is a Professor of Electromechanics at the Faculty of Science and Technology, Larbi Tebessi University, Tebessa, Algeria. He is also the head of the Environmental Laboratory at the Institute of Mines in Tebessa. His recent research focuses on optimizing drilling parameters in the mining industry, with a particular interest in environmental studies. He can be contacted at email: messaoud.louafi@univ-tebessa.dz.

**Sihem Ghoudelbourk** is born in Annaba on 25 may 1969. She is currently residing in Annaba City; she graduated with a diploma in Electrotechnical Engineering degree from Badji Mokhtar University of Annaba in 1994. The master's degree in 2012. She received her Ph.D. in power systems in 2016, and currently works at the Department of Electrical Engineering of the University of Badji Mokhtar Annaba, Algeria. Her main current research interests include renewable energy power electronics, and electrical machines. She participated in several conferences and published several papers. She can be contacted at email: sihem.ghoud-lbourk@univ-annaba.dz.